Supporting information

1. Experimental

1.1. Synthesis of ligand and catalyst

Synthesis of ligand

The synthesis procedure of bpyOH-CpIr is shown below. The bpydc-OH ligand (step1-step4) was synthesized according to previous literature.[1]

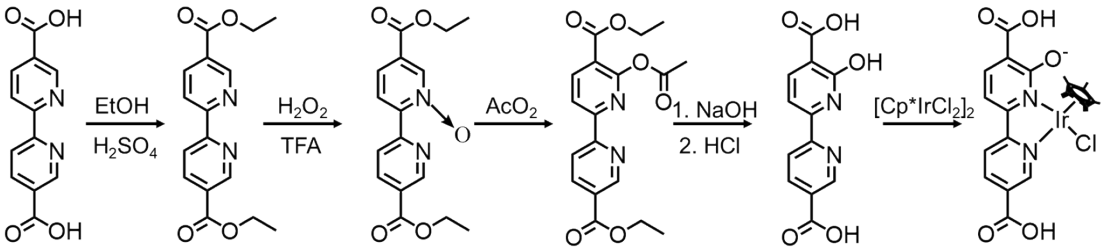

1g of 2,2'-bipyridine-5,5'-dicarboxylic acid (bpydc) was added in 60 mL of ethanol, and then 4 mL of H_2SO_4 was slowly added to the mixture. The mixture was refluxed at 120℃ under magnetic stirring for 15 h. 80 mL of water was added to the mixture, and then ammonia solution was added to neutralize the solution. Diethyl-2,2'-bipyridine-5,5'-dicarboxylate was extracted with methylene chloride. The pale solid was obtained by evaporating solvent (yield, 89%). ^{1}H-NMR (500 MHz, DMSO-d_6): δ 9.29 (s, 2H), 8.57 (d, J = 8.3 Hz, 2H), 8.43 (dd, J =8.3, 2.1 Hz, 2H), 4.45 (q, J = 7.1 Hz, 4H), 1.44 (t, J = 7.1 Hz, 6H).

1.8 g of diethyl-2,2'-bipyridine-5,5'-dicarboxylate was added in 10 mL of TFA, and 613 μL of 30% H_2O_2 (molar ratio of 1:1) was then added. The mixture was stirred at 25℃ for 2h. After that, 5% K_2CO_3 solution was added to obtain white precipitate, which was

collected by centrifugation. The solid was washed with water and dried under vacuum. ^{1}H-NMR (500 MHz, DMSO-d_6): δ 9.32 (s, 1H), 9.15 (d, J = 8.4 Hz, 1H), 8.91 (s, 1H), 8.48 –8.36 (m, 2H), 7.94 (d, J = 8.4 Hz, 1H), 4.46 (m, 4H), 1.44 (m, 6H).

1g of diethyl-2,2'-bipyridine-5,5'-dicarboxylate-N-oxide was added to 30 mL of acetic anhydride and refluxed at 137℃ for 35h. After removing solvent by distillation, the crude product was purified with column chromatography with CH_2Cl_2 to obtain 6-hydroxyl-diethyl-2,2'-bipyridine-5,5'-dicarboxylate acetate in 59% yield. ^{1}H-NMR (500 MHz, DMSO-d_6): δ9.28 (dd, J = 2.2, 0.9 Hz, 1H), 8.57 – 8.47 (m, 3H), 8.41 (dd, J = 8.2, 2.1 Hz, 1H), 4.42 (dq, J = 27.3, 7.1 Hz, 4H), 2.44 (s, 3H), 1.42 (dt, J = 13.8,7.1 Hz, 6H).

300mg of 6-hydroxyl-diethyl-2,2'-bipyridine-5,5'-dicarboxylate acetate was added in of 6 mL of 3 M NaOH solution and 9 mL of ethanol, 5 mL of THF, and the mixture was stirred at 90℃ for 4h. After removing the organic solvents, deionied water was added. The solution was then acidified to pH = 1 with HCl to obtain yellow precipitate. Finally, the solid was washed with water and dried under vacuum to obtain 6-hydroxyl-diethyl-2,2'-bipyridine-5,5'-dicarboxylic acid (yield 90%). ^{1}H-NMR (400 MHz, DMSO-d_6): δ 8.77 (s, 1H), 8.11 (dd, J = 8.3, 2.2 Hz, 1H), 7.87 (d, J = 8.7 Hz,1H), 7.48 (d, J = 7.4 Hz, 1H), 6.95 (d, J = 7.4 Hz, 1H).

$[Cp^*IrCl_2]_2$ (212mg) and $AgNO_3$(180.2mg) was added in 20mL of H_2O and stirred at 40℃ overnight. After removing the AgCl precipitate, 143mg of bpydc-OH was added

to the solution. The obtained mixture was treated with NaOH to pH = 7 and was stirred at 40℃ for 24h. The solution was then acidified to pH = 1 with HCl. The resulting orange precipitate was collected and washed with water and dried under vacuum. ^{1}H-NMR (500 MHz, DMSO-d_6): δ 9.92 (s, 1H), 8.48 (d, J=8.1 Hz, 1H), 8.40(d, J=8.1Hz, 2H), 7.77(d, J=7.5 Hz,1H), 1.59(s, 15H).

Synthesis of UiO-bpyOH-IrCp

$ZrCl_4$ (99.99% 120 mg) and benzoic acid (1.5g) were dissolved in 10 mL of DMF in a Pyrex vial using sonication for 3min, and the linker bpy-OH-IrCp (76 mg) and bpdc (95 mg) were dissolved in 10 mL of DMF by sonication for 3min. After mixing the two solutions, the Pyrex vials were kept in an oven at 120℃ for 72 h. Yellow precipitates were collected by centrifugation after cooling to room temperature and were washed with DMF three times to remove unreacted precursors and with acetone 6 times to remove DMF and then dried at 60℃ under vacuum.

Synthesis of UiO-bpyOH-IrCp-Sc

UiO-bpyOH-IrCp-Sc was synthesized from UiO-bpyOH-IrCp by metalation. $Sc(SO_3CF_3)_3$ (135mg) was dissolved in 20mL of THF. UiO-67-Ir (65 mg) was added to the $Sc(SO_3CF_3)_3$ solution. The resulting suspension was stirred at 60℃ for 20h and the solid was then centrifuged out and washed with THF for 6 times. The metalated MOFs were then dried under vacuum.

Synthesis of UiO-bpy

$ZrCl_4$ (120 mg) and benzoic acid (1.5g) were dissolved in 10 mL of DMF in a Pyrex vial using sonication for 3min, and the linker bpydc (126 mg) were dissolved in 10 mL of DMF by sonication for 3min. After mixing the two solutions, the jars were kept in an oven at 120℃ for 72 h. White solid was then centrifuged out and washed with DMF 3 times and washed with acetone 6 times. Finally, it was dried at 60℃ under vacuum.

Synthesis of UiO-bpyOH

$ZrCl_4$ (120 mg) and benzoic acid (1.5g) were dissolved in 10 mL of DMF in a Pyrex vial using sonication for 3min, and the linker bpdc (63 mg) and bpyOH (63 mg) were dissolved in 10 mL of DMF by sonication for 3min. After mixing the two solutions, the jars were kept in an oven at 120℃ for 72 h. White solid was then centrifuged out and washed with DMF for 3 times and washed with acetone 6 times. Finally, It was dried at 60℃ under vacuum.

Synthesis of UiO-bpyOH-IrCl3 and UiO-bpy-IrCl3

$IrCl_3 \cdot XH_2O$ (100mg) was added to 20mL of acetonitrile. And then UiO-bpy (200 mg) or UiO-bpyOH (200 mg) was added to the above mixture. The resulting suspension was stirred at 80℃for 20h in Ar. After that, solid was centrifuged out and washed with acetonitrile for 4 times. The metalated MOFs were then dried under vacuum.

1.2. Catalyst characterization

^{1}H-NMR spectra were recorded on a Bruker NMR DPX-500 spectrometer. The number

of scans was 32. Powder X-ray diffraction (PXRD) experiments were carried out on a Bruker D8 Venture (Cu *Ka* radiation). The X-ray diffraction patterns were collected from $2\theta = 3^{o}$ to 80^{o}. The voltage and current were operated at 40 kV and 300 mA, and the scanning speed was 10^{o} /min. N_2 adsorption-desorption isotherms were measured with a Micromeritics instrument (ASAP2040). Before N_2 physical adsorption, the sample (~0.1 g) was degassed at 100℃ for 6 h under the vacuum. The specific surface area was calculated according to the BET method. Inductively coupled plasma-mass spectrometry (ICP-MS) measurements were undertaken on an ELAN ICP-DRC-qMS (PerkinElmer, SCIEX, Canada) instrument equipped with a concentric pneumatic nebulizer (Meinhard) and a Cyclonic spray chamber. Samples were diluted in 5% HNO3 matrix and analyzed with a Tb internal standard against a six-point standard curve over the range from 1 ppm to 100 ppm. Transmission electron microscope (TEM, Tecnai G2 F30 S-Twin, Philips-FEI Co.) and EDX mapping was used to observe the morphologies of the catalysts before and after catalytic reaction and metal element dispersion. The powders were ultrasonically dispersed in the ethanol solution to form a suspension, and it was doped to the porous copper grid coated with carbon film for TEM observation. X-ray photoelectron spectroscopy (XPS, Kratos AXIS ULtra DLD) was used to analyze the surface chemical states of the catalysts. The C_{1s} peak at 284.6 eV was used as a charge correction reference in this study. For NH_3 temperature-programed desorption (NH_3-TPD), 60 mg of the samples were placed in a quartz reactor and purged by Ar for 1h at 150℃. When the temperature decreased to 50℃, a flow of NH_3-Ar(5%) was fed into at 30 ml/min for 1h, and then the catalyst was

purged by Ar for 1h. The temperature was linearly increased from 50℃ to 300℃ at 5℃/min in Ar, and NH_3-TPD profiles were recorded by thermal conductivity detector (TCD)

1.3. Catalytic reaction

Catalytic performance of the alcohol dehydrogenation was tested in a Schlenk tube. 30mg of catalyst and 1mL of alcohols were loaded to the 10mL Schlenk tube and heated to 150℃ or 120℃ under stirring for 20h by using an aluminum heating block. After catalytic reaction, the Schlenk tube was allowed to cool to room temperature and then kept in an ice-water bath for 20 min. Then 1mL of Ar as an internal standard was added. The gas composition was analyzed by using a gas chromatograph (GC) equipped with a thermal conductivity detector (TCD) and a flame ionization detector (FID) and the liquid production was analyzed by GC-Mass.

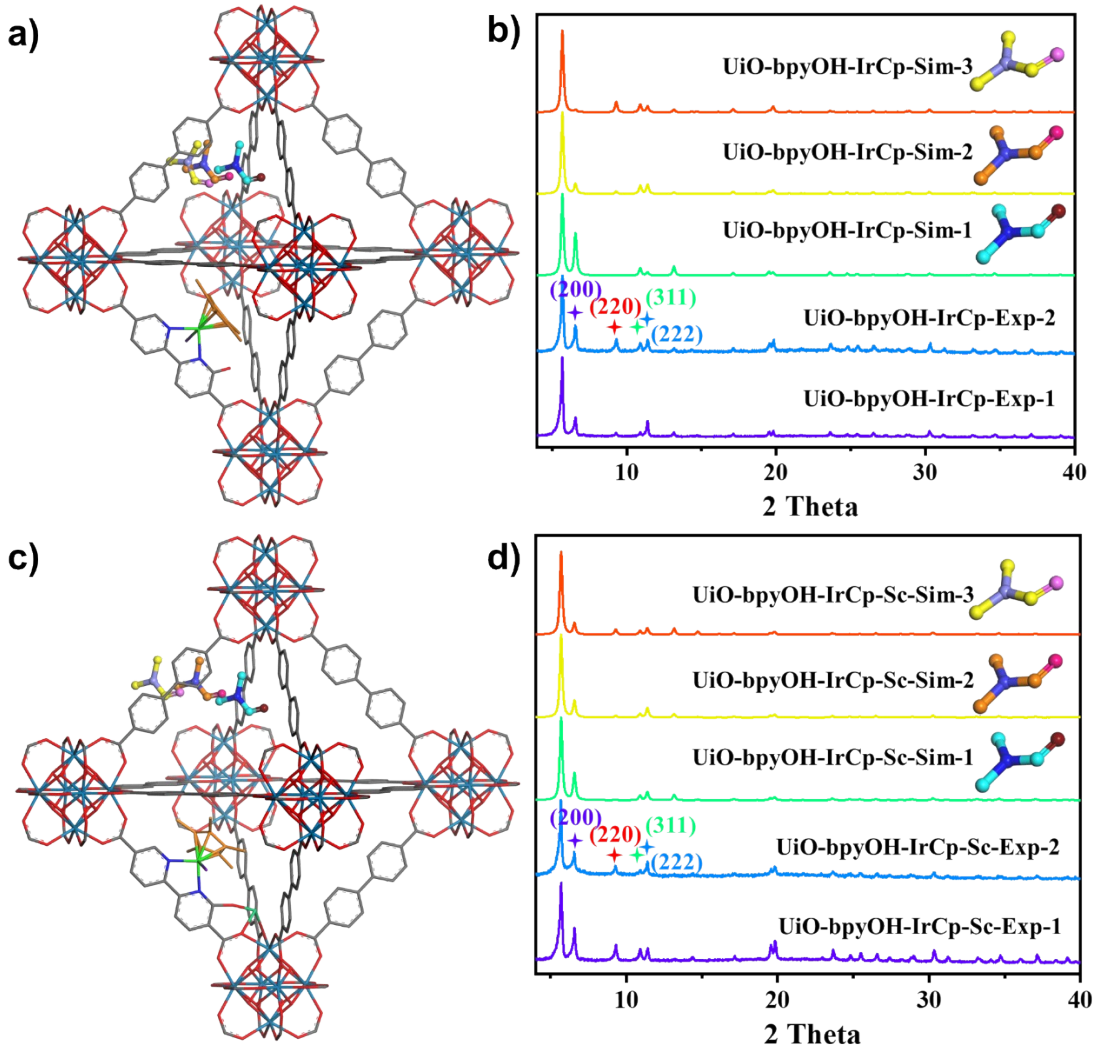

Figure S1 Modelling PXRD patterns of the UiO-bpyOH-IrCp and UiO-bpyOH-IrCp-Sc with model containing DMF molecules at different positions.

Both UiO-bpyOH-IrCp and UiO-bpyOH-IrCp-Sc crystallize in the cubic space group Fm$\bar{3}$m with the unit cell parameters close to 26.896 Å. Based on the 1H NMR spectra, the UiO-bpyOH-IrCp contains about 12 DMF molecules located in the octahedral pores per unit cell, while UiO-bpyOH-IrCp-Sc contains 4 DMF molecules. By adjusting the location of DMF molecules in the pores (S1a & 1c), the intensity of non-overlapping reflections with indexes (200), (220), (311) and (222) changes significantly which is consistent with the experimental observation.

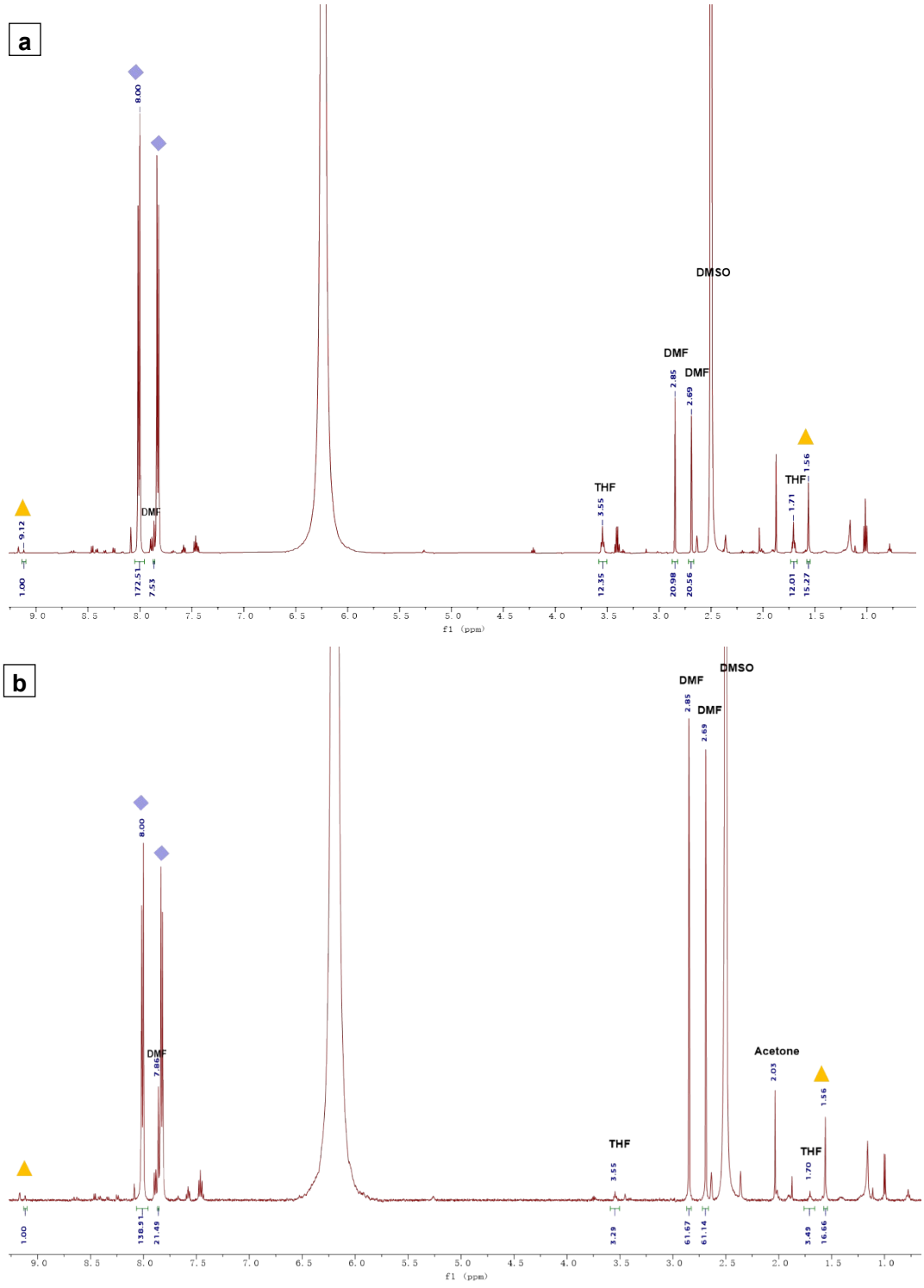

Figure S2. ^{1}H-NMR spectrum of UiO-bpyOH-IrCp-Sc(a) and UiO-bpyOH-IrCp(b) digested in D_3PO_4-D_2O/DMSO-d6. Peaks are assigned to bpdc(◆) and bpyOH-IrCp(▲)

UiO-bpyOH-IrCp：n(BPDC) : n(DMF) = 2 : 1 was obtained from the integrations.
UiO-bpyOH-IrCp-Sc：n(BPDC) : n(DMF) = 6 : 1 was obtained from the integrations.

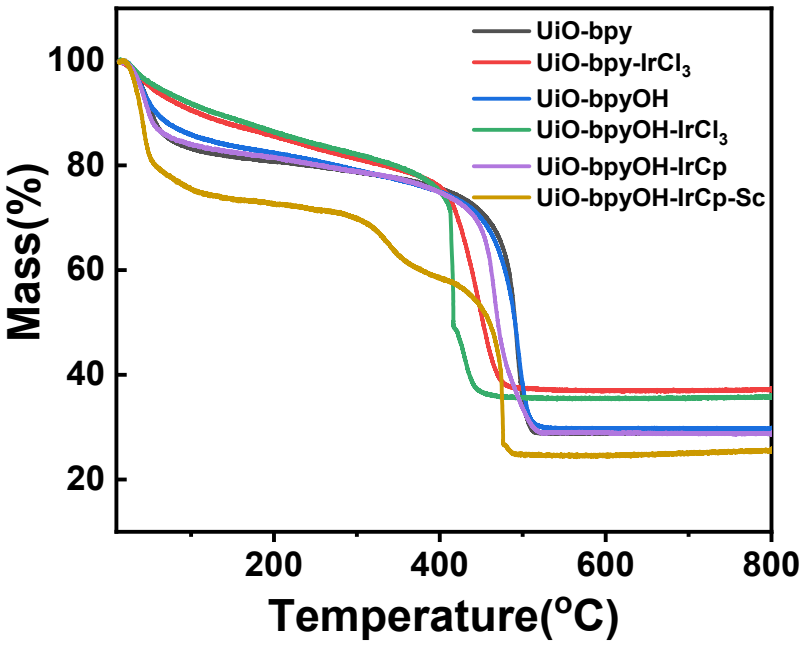

Figure S3. The thermogravimetric analysis (TGA) of prepared samples

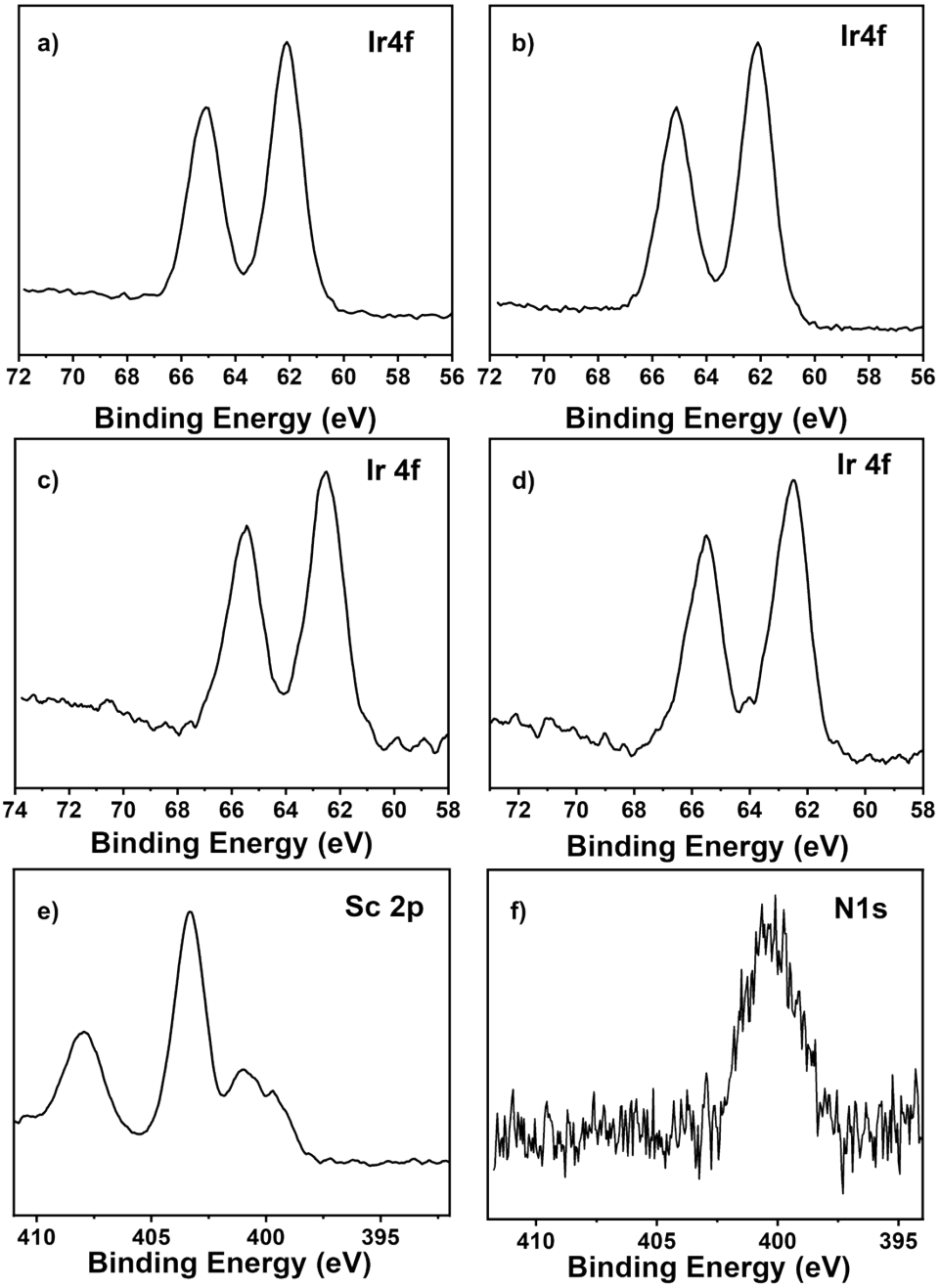

Figure S4. Ir_{4f}-XPS of UiO-bpy-$IrCl_3$ (a), UiO-bpyOH-$IrCl_3$ (b), UiO-bpyOH-IrCp (c), UiO-bpyOH-IrCp-Sc (d); Sc_{2p}-XPS of UiO-bpyOH-IrCp-Sc(e); N_{1S}-XPS of UiO-bpyOH-IrCp(f)

Two peaks appeared at ~62.5eV and ~65.5eV in in the XPS spectra of both UiO-bpyOH-IrCp and UiO-bpyOHIrCp-Sc, which are assigned to the $Ir^{3+}{}_{4f7/2}$ and $Ir^{3+}{}_{4f5/2}$. [2] For the UiO-bpy-$IrCl_3$ and UiO-bpyOH-$IrCl_3$, the $Ir^{3+}{}_{4f7/2}$ peak appears at lower binding energy of ~62.1eV, possibly due to the absence of Cp* ligand and the presence of coordinated

Cl^-. The Sc_{2p} peaks at ~403.3eV and ~407.9eV can be ascribed to $Sc^{3+}{}_{2p3/2}$ and $Sc^{3+}{}_{2p1/2}$, respectively[3], in the spectrum of the UiO-bpyOHIrCp-Sc. There was also a small peak at ~400eV in the spectrum, which is related to N1s of the bpyOH ligand.

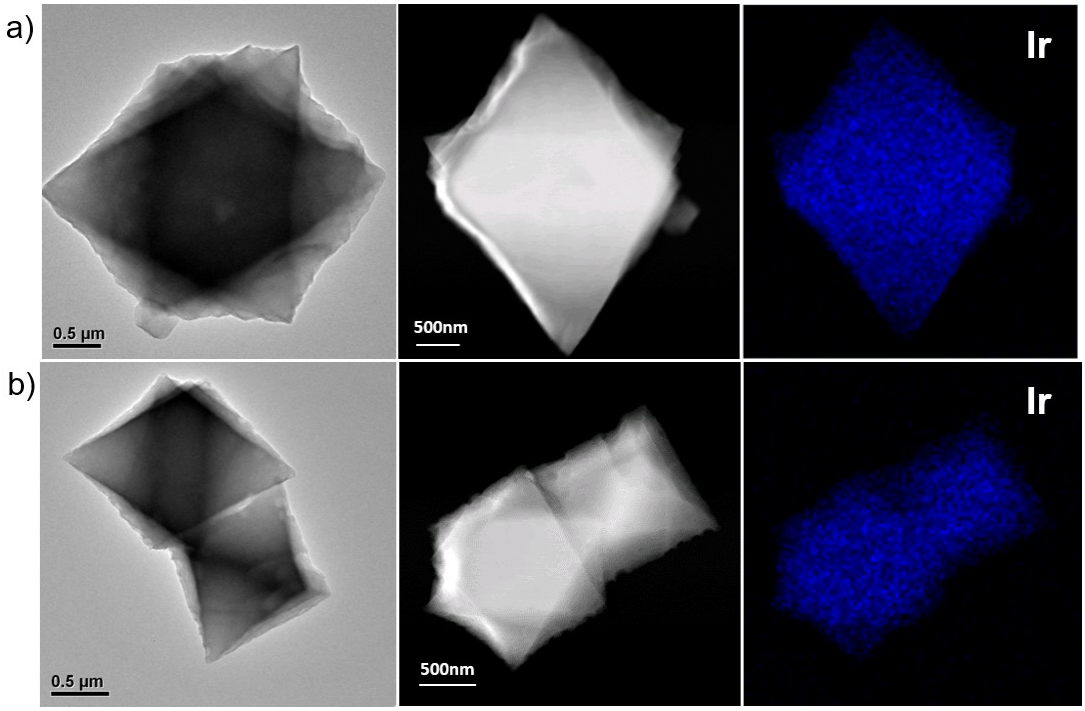

Figure S5. TEM image, dark-field TEM image and the corresponding EDS mapping of UiO-bpy-$IrCl_3$ (a), UiO-bpyOH-$IrCl_3$(b)

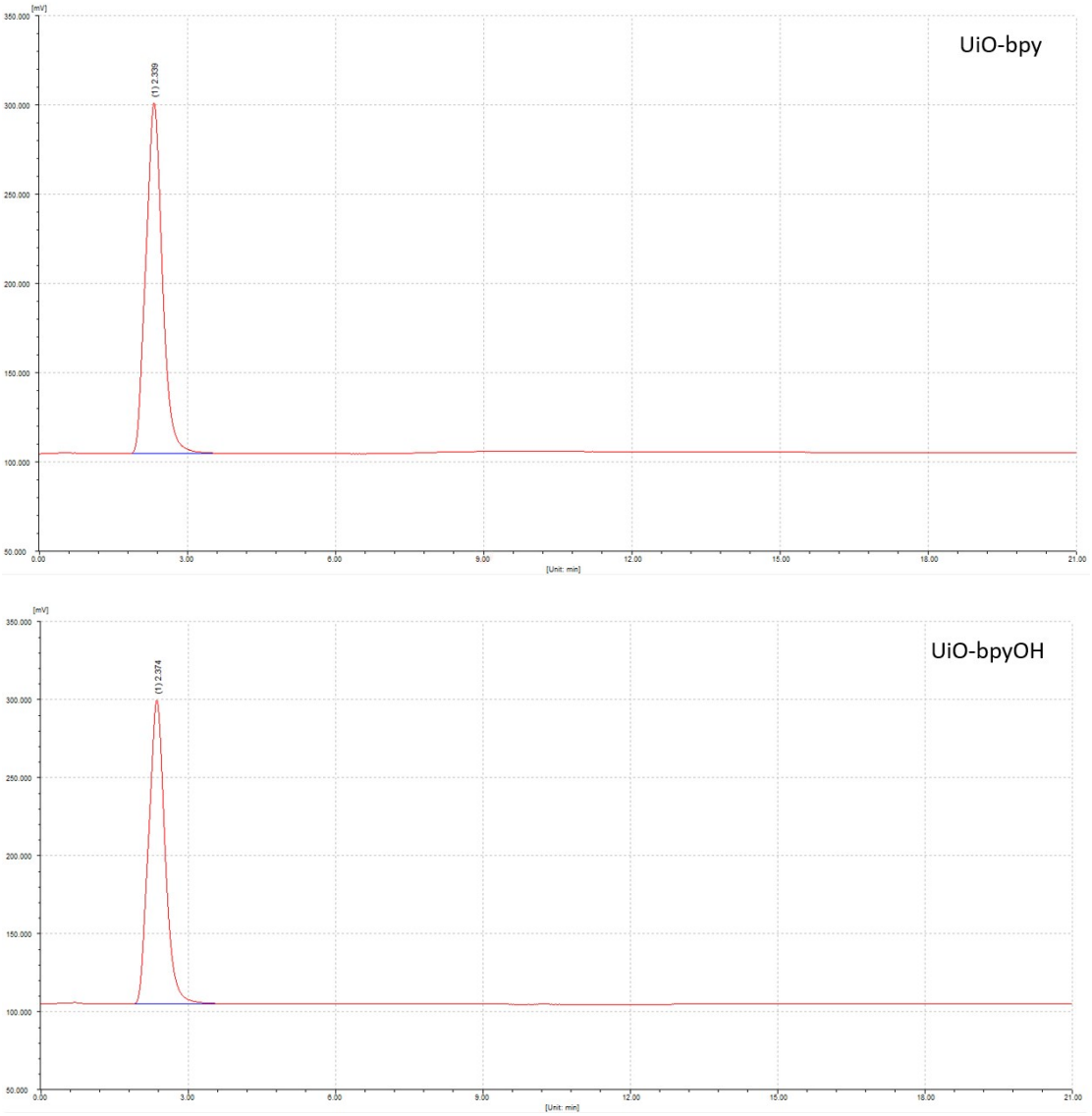

Figure S6. The GC analysis results of UiO-bpyOH and UiO-bpy for EG dehydrogenation at 150℃(the retention time of H_2 is 0.7min; the peak at 2.3 min is from N_2)

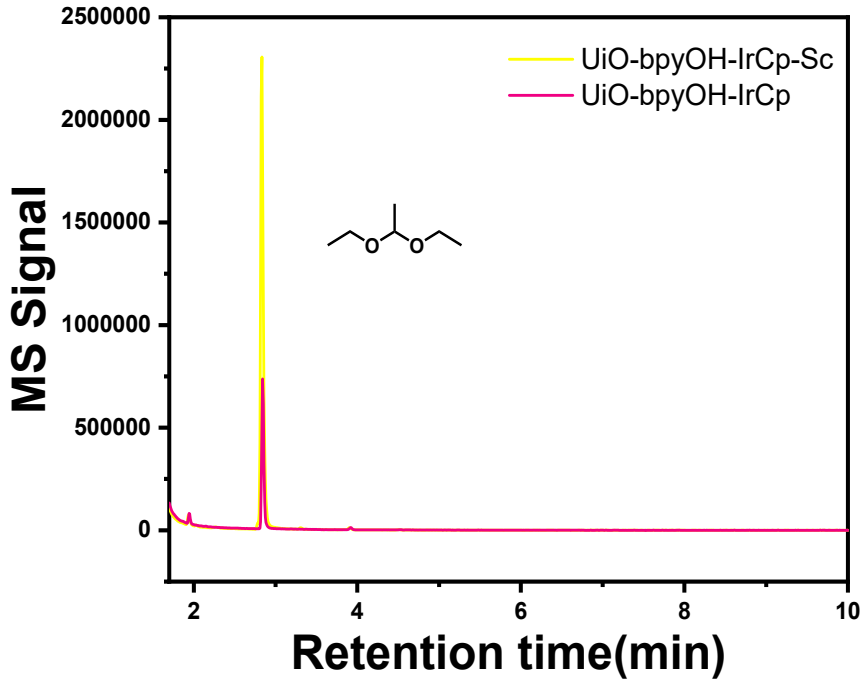

Figure S7 GC-MS of the liquid production of ethanol dehydrogenation over UiO-bpyOH-IrCp-Sc and UiO-bpyOH-IrCp

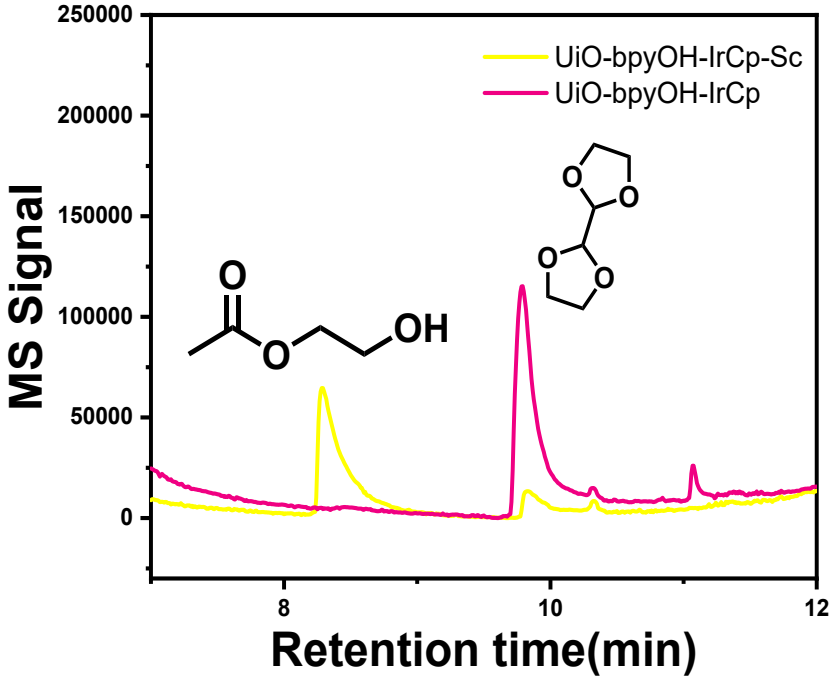

Figure S8 GC-MS of the liquid production of ethylene glycol dehydrogenation over UiO-bpyOH-IrCp-Sc and UiO-bpyOH-IrCp

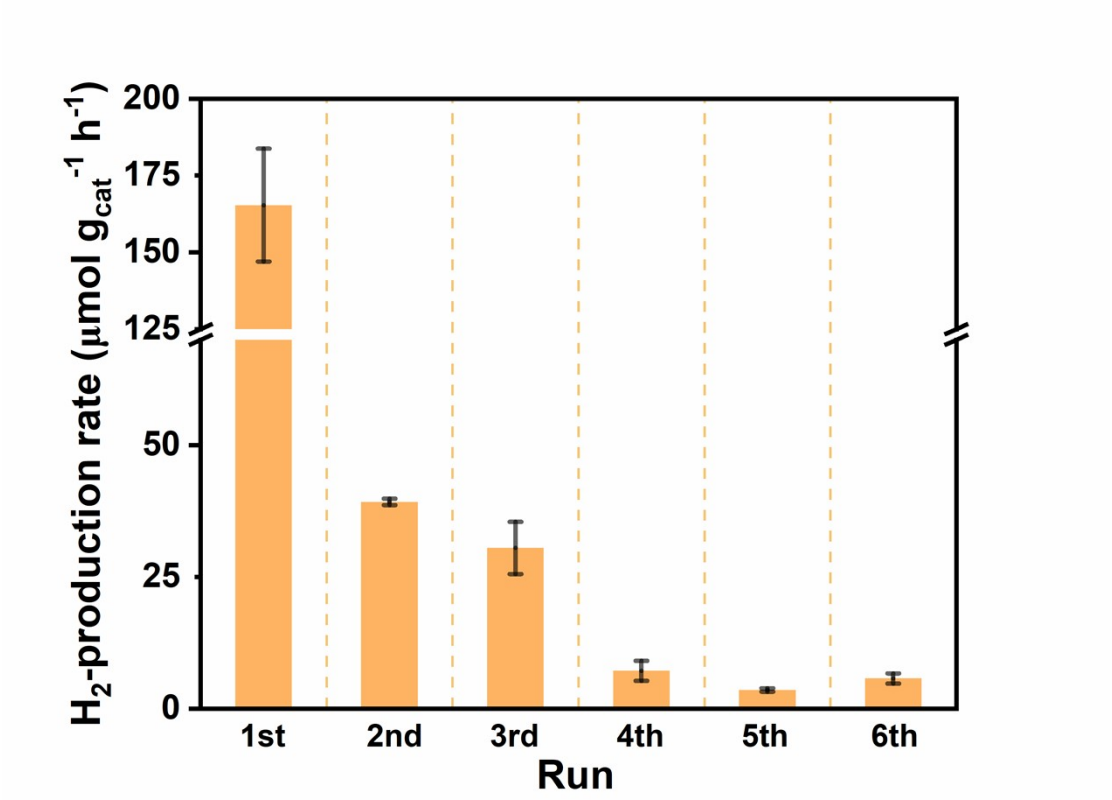

Figure S9 Reusability of UiO-bpyOH-IrCp-Sc in the dehydrogenation of ethylene glycol (150℃)

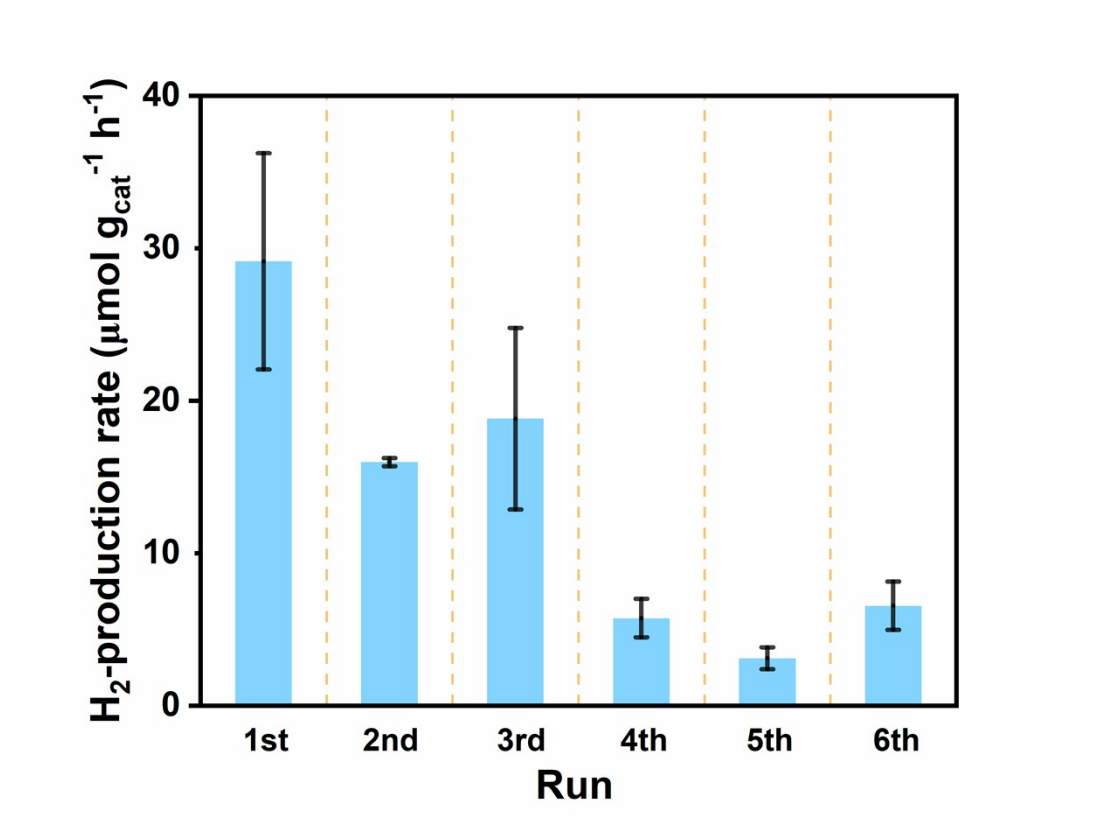

Figure S10 H_2 production rate for the UiO-bpyOH-IrCp recycling experiments (EG; 150℃)

Table S1 ICP-MS results of catalysts and control samples

Sample	Ir (wt%)	Sc (wt%)	Ir/Zr (mol/mol)	Sc /Zr (mol/mol)	Ir/Sc (mol/mol)
UiO-bpy-$IrCl_3$	26.66(±1.91)		0.497(±0.022)	-	-
UiO-bpyOH-$IrCl_3$	14.37(±0.21)		0.376(±0.015)	-	-
UiO-bpyOH-IrCp	1.94(±0.23)	0.021	0.061(±0.005)	0.003	-
UiO-bpyOH-IrCp-Sc	1.74(±0.04)	0.43(±0.02)	0.059(±0.005)	0.062(±0.004)	0.94(±0.015)
UiO-bpy-Sc	-	0.12(±0.01)	-	0.012(±0.003)	-
UiO-bpyOH-Sc	-	0.05(±0.001)	-	0.005 (±0.0001)	-

Table S2 H_2 productivity of different catalysts for ethylene glycol dehydrogenation.

Cat	H_2 productivity ($\mu mol\ g^{-1}\ h^{-1}$)	Reaction condition	References
Ni-Mg-MOF-74	134000	250℃	4
Pd/TiO_2	38400	O_2 = 0.001 atm UV light photoreaction	5
Ni/CeO_2-Al_2O_3	15528	250℃	6
Ni/CeO_2	11736	250℃	6
Ni-Pt/Al_2O_3	6262	600℃	7
Ru pincer complex	2092	150℃ (homogeneous reaction)	8
UiO-bpyOH-IrCp-Sc	186	150℃ (neat reaction)	This work

1. B. An, L. Zeng, M. Jia, Z. Li, Z. Lin, Y. Song, Y. Zhou, J. Cheng, C. Wang and W. Lin, *J. Am. Chem. Soc.*, 2017, **139**, 17747-17750.
2. T. Zhang, K. E. deKrafft, J. L. Wang, C. Wang and W. Lin, *Eur. J. Inorg. Chem.*, 2014, **4**, 698-707.
3. R. Rahman, J. P. Klesko, A. Dangerfield, M. Fang, J.S. M. Lehn, C. L. Dezelah, R. K. Kanjolia, Y. J. Chabal, J. Vac. Sci. Technol. A, 2019, 37, 011504-1-011504-6.
4. J. L. Snider, J. Su, P. Verma, F. El Gabaly, J. D. Sugar, L. Chen, J. M. Chames, A. A. Talin, C. Dun, J. J. Urban, V. Stavila, D. Predergast, G. A. Somorjai and M. D. Allendorf, *J. Mater. Chem. A*, 2021, **9**, 10869-10881.
5. A. K. Wahab, M. A. Nadeem and H. Idriss, *Front. Chem.,* 2019, 780-796.
6. X. l. Zhao, Y. LÜ, W. Liao, M. Jin and Z. Suo, *J. Fuel Chem. Technol.*, 2015, **43**, 581-588.
7. A. Larimi and F.qi Khorasheh, *Renew. Energ.*, 2018, **128**, 188-199.
8. Y. Q. Zou, N. von Wolff, A. Anaby, Y. Xie and D. Milstein, *Nat Catal,* 2019, **2,** 415-422.